Journal of Materials Chemistry C

Novel Branched Nanostructures Based on Polyhedral Oligomeric Silsesquioxanes and Azobenzene Dyes Containing Different Spacers and Isolation Groups

Journal:	*Journal of Materials Chemistry C*
Manuscript ID	TC-ART-01-2018-000223.R1
Article Type:	Paper
Date Submitted by the Author:	23-Feb-2018

Complete List of Authors:	Tkachenko, Ihor; Institute of Macromolecular Chemistry of the National Academy of Sciences of Ukraine, Department of Chemistry of Oligomers and Netted Polymers Kobzar , Yaroslav; Institute of Macromolecular Chemistry of the National Academy of Sciences of Ukraine, Department of Chemistry of Oligomers and Netted Polymers Korolovych, Volodymyr; Georgia Institute of Technology, School of Materials Science and Engineering Stryutsky, Alexandr ; Institute of Macromolecular Chemistry of the National Academy of Sciences of Ukraine, Department of Chemistry of Oligomers and Netted Polymers Matkovska, Liubov ; Institute of Macromolecular Chemistry of the National Academy of Sciences of Ukraine Shevchenko, Valery; Institute of Macromolecular Chemistry of the National Academy of Sciences of Ukraine, Department of Chemistry of Oligomers and Netted Polymers Tsukruk, Vladimir; Georgia Institute of Technology, School of Materials Science and Engineering

Novel Branched Nanostructures Based on Polyhedral Oligomeric Silsesquioxanes and Azobenzene Dyes Containing Different Spacers and Isolation Groups

Ihor M. Tkachenko,[a] Yaroslav L. Kobzar,[a] Volodymyr F. Korolovych,[b] Alexandr V. Stryutsky,[a] Liubov K. Matkovska,[a] Valery V. Shevchenko,*[a] Vladimir V. Tsukruk*[b]

[a] Institute of Macromolecular Chemistry, National Academy of Sciences of Ukraine, Kharkivske shosse 48, Kyiv, 02160, Ukraine

[b] School of Materials Science and Engineering, Georgia Institute of Technology, Atlanta, Georgia, 30332, United States

*Corresponding authors' e-mail: valpshevchenko@gmail.com (Valery V. Shevchenko) and vladimir@mse.gatech.edu (Vladimir V. Tsukruk)

Abstract

The great interest in smart light-responsive material led to the development of hybrid star-shaped nanostructures combining organic azobenzene dyes with polyhedral oligomeric silsesquioxanes (Azo-POSS). Herein we present two approaches to fabricating the azo-functionalized POSS compounds with the desired characteristics: (1) synthesis of branched Azo-POSS structures based on azo dyes possessing flexible spacers of different chemical natures and lengths between the inorganic POSS core and the azobenzene branches, and (2) an approach that was fist applied to Azo-POSS systems – synthesis of the Azo-POSS conjugates with isolation groups (they minimize undesired chromophore-chromophore interaction) in the azobenzene fragments and the constant short spacer between azo dyes and medium. The first one was synthesized from azo dyes containing hexenyloxy-, allyloxy-ethoxypropoxy- and tetramethyl-disiloxanyl-propoxy substituents, while the second one was prepared from allyl-functionalized azo-based chromophores with changeable isolation groups (hydroxymethylene-, trimethylsiloxymethylene- and pentafluorophenoxymethylene-groups). According DSC analysis Azo-POSS based on hexenyloxy-substituted dye has crystalline domains whereas all other Azo-POSS compounds are amorphous. We found that robust and ultrathin films with thicknesses of around 60 nm and low refractive indices (ca. 1.46) can be fabricated from all Azo-POSS branched conjugates. It was demonstrated that surface roughness of Azo-POSS films can be significantly minimized by the attachment of azo dyes having side isolation groups into

the POSS core. Moreover, for Azo-POSS molecules with isolation groups in azobenzene units, we observed the significant decrease of the *trans-cis* photoisomerization rate in solution compared to other obtained star-shaped Azo-POSS systems. At the same time, the photoisomerization rates of synthesized here Azo-POSS conjugates in films are almost the same. These results indicate that the presence of the isolation groups effectively prevents inter- and intramolecular aggregation of azobenzene chromophores attached to the POSS core in solid state.

Keywords: Azo dyes, POSS, star molecules, hydrosilylation, photoisomerization

Introduction

Azobenzene (azo)-containing chromophores are very attractive systems due to their *trans*-to-*cis* photoisomerization [1-13]. Reversible photoisomerization from the thermodynamically more stable *trans* isomer to the *cis* isomer can be induced by irradiation with UV light (~365 nm). Hence, the investigation of azo-containing dyes has been increasing because of their potential applications in optical and electronic switching, non-linear optical devices and information storage [1-21].

However, the low thermal stability and high ability to aggregation in solid phase of the azobenzene dyes have limited their applications in devices [22-27]. The conjugation of organic chromophores to polyhedral oligomeric silsesquioxane (POSS) core results in novel hybrid materials with high thermo-, mechano- and photostability, enhanced optical, nonlinear optical and dielectric properties, as well as good liquid crystal phase stability. Furthermore, the aggregation effect is effectively suppressed due to the covalent binding of organic chromophores to the inorganic POSS cage [27-41]. Additionally, it has been found that molecules with POSS core and azobenzene dye arms (Azo-POSS) are able to form stable, uniform, smooth, and ultrathin films. Importantly, the reversible photoisomerization of azobenzene units still occurs in such stable Azo-POSS films [42, 43].

However, inorganic POSS core does not always prevent chromophores aggregation in solid state [43, 44]. For example, recently two star-shaped Azo-POSS compounds with different spacer lengths between the inorganic core and the azobenzene moiety were synthesized [42, 43]. It was shown the branched conjugate with a long spacer (1.87 nm) between a dimethylsilyl unit of the core and the azobenzene fragments (Azo-POSS-long) undergoes photoisomerization in solution but not in an ultrathin solid film due to the aggregation of azobenzene fragments [43]. The thin film of Azo-POSS conjugate with a shorter spacer (0.7 nm) between the core and the azobenzene moieties (Azo-POSS-short), however, exhibited a pronounced change in intensity of the $\pi-\pi^*$ transition at 350 nm, indicating efficient *trans*-to-*cis* isomerization [42, 43]. Moreover, Azo-POSS-short conjugate exhibited a large refractive index variation when irradiated with UV light (higher than that of simple azobenzene embedded in a polymer matrix) and it was found significant, reversible, and repeatable shifts in localized surface plasmon resonance peak position upon alternating irradiation of the Azo-POSS-short/silver nanocube composite film with UV and visible light [43]. On the other hand, decreasing of the spacer length leads to

relatively high crystallinity of Azo-POSS-short system and, consequently, Azo-POSS-short forms a relatively rough film that appears in lack of the characteristics. Whereas it is known, that organic films that are smooth and homogeneous over large areas show low optical losses and have advanced optic, optoelectronic and protective properties [45-47].

Therefore, it is crucial to regulate the spacer length between the POSS inorganic core and the azobenzene moiety in order to obtain processable materials with suppressed crystallization and stacking ability as well as with high nanocomposite film-forming ability and preserved reversible photoisomerization. On the other hand, incorporation of side bulky groups into azo chromophore with the constant short spacer length between azo dyes and medium (for example polymer and POSS) can suppress crystallization of such azo-containing materials. And more importantly, these chemical bulky groups can serve as so-called suitable isolation groups which are introduced to decrease the harmful intermolecular dipole-dipole and the *π–π* stacking interaction of chromophores and, consequently, prevent dye aggregations. [48-53]. However, nowadays the isolation groups are widely used to create, as a rule, only nonlinear optical materials where *trans-cis* photoisomerization is not necessary.

In fact, to date, the photoisomerization behavior of star-shaped Azo-POSS structures have mostly been studied in solvent media [27, 34, 40, 42, 43]. Additionally, for example, Miniewicz et al. demonstrated the reverse photochromism of polymeric composite matrix with dispersed azo-functionalized POSS nanoparticles (up to 15% w/w) [37]. Next, Guo et al. showed that *trans-cis* photoisomerization of cross-linked Azo-POSS occurred, but (that is reasonable) only after sample swelling in toluene [26]. Thus, to the best of our knowledge, our recent works [42, 43] on photoisomerization in films prepared from exceptionally individual Azo-POSS nanostructures (Azo-POSS-short and Azo-POSS-long) are the first studies in this field. However, information is still lacking regarding the influence of the length and chemical nature of the flexible spacers between the POSS core and the active azochromophores as well as chemical structures of the azo dyes on different properties of Azo-POSS in both solvent and, especially, films.

The current work represents a comprehensive approach for the synthesis of highly substituted Azo-POSS structures with the ability of the obtained Azo-POSS systems to form stable, uniform, smooth, and ultrathin films from azo dyes containing hexenyloxy-, allyloxy-ethoxy-propoxy- and tetramethyl-disiloxanyl-propoxy substituents as well as allyl-

functionalized azobenzene derivatives with changeable isolation groups (hydroxymethylene- or pentafluorophenoxymethylene groups). We demonstrated that thermal and film-forming properties as well as refractive indices of the obtained brunched Azo-POSS nanostructures mainly depend on the variation of chemical natures and lengths of spacers that connect inorganic POSS core with azobenzenes and directly chemical structures of azo dyes (with or without isolation groups). Notably, the side isolation hydroxymethylene- or pentafluorophenoxymethylene groups are effective for preparation of uniform amorphous films with low scattering and, more importantly, such groups suppress aggregation of azobenzenes. Interestingly, that the *trans-cis* photoisomerization of the Azo-POSS conjugates (which were synthesized from azobenzenes without isolation groups) in chloroform solution occurs faster than isomerization of the Azo-POSS possessing isolation groups in their azobenzene arms, whereas the photoisomerization rates of all synthesized Azo-POSS conjugates in films are almost the same.

Results and Discussion

Synthesis of Azo-POSS conjugates. In a previous communication we have reported the first successful synthesis of reactive azo dyes based on 4-phenylazophenol, containing hexenyloxy- (**1**), allyloxy-ethoxy-propoxy- (**2**) and tetramethyl-disiloxanyl-propoxy substituents (**3**). Additionally, allyl-functionalized azo-based chromophores with changeable isolation groups (hydroxymethylene- (**4**) and pentafluorophenoxymethylene groups (**5**)) were obtained [54]. The chemical structures of these azo dyes are presented in Figure 1.

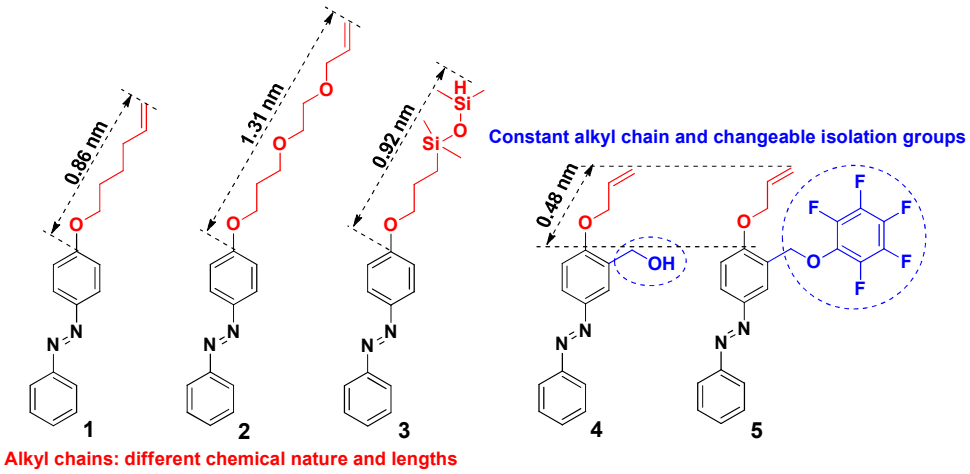

Figure 1. The chemical structures of azo dyes with different alkyl chains and isolation (hydroxymethylene- and pentafluorophenoxymethylene) groups used in this study and the lengths of their alkyl chains.

Notably, hydroxymethylene groups of dye **4** can serve not only as an isolation groups, but also as a highly versatile platform for further functionalization. Thus, we used hydroxyl functional groups in the chemical structure of dye **4** for its modification with perfluoroaromatic ring (dye **5**). It is known that perfluoroaromatic rings are electropositive, which could lead to reversible self-assembly between the non-fluorinated aromatic units and the perfluoroaromatic units (Ar-Ar_F interactions) [55].

The alkyl tail lengths of azo compounds **1** (0.86 nm), **2** (1.31 nm), **3** (0.92), **4** and **5** (both 0.48 nm) were calculated from molecular models [54]. Although the alkyl tail lengths of azo dyes **1** and **3** were comparable, they have different chemical structures. We suggest that the synthesized azo structures **1-5** with different length of alkyl chains and isolation groups can be considered for the synthesis of novel branched organic-inorganic azo-polyhedral oligomeric silsesquioxane conjugates with suppressed crystallization and aggregation ability.

Furthermore, in order to elucidate the role of azobenzene conjugation, we synthesized a series of highly substituted Azo-POSS structures based on azobenzenes **1-5** via hydrosilylation coupling (Scheme 1 and 2). Hydrosilylation is a reliable method for Si−C bond formation under Pt(0) catalysis. For the synthesis of **Azo-POSS-1** and **Azo-POSS-2** with different spacers, an octakis-(dimethylsilyloxy)silsesquioxane (**POSS-H**) was chosen as an initial scaffold. As dyes, we used azobenzenes **1** and **2** containing flexible and reactive hexenyloxy- and allyloxy-ethoxy-propoxy fragments respectively. Having a functionalized dye with organic-inorganic flexible spacer and terminal reactive Si-H group (azo dye **3**), we moved to preparation of **Azo-POSS-3** conjugate using octavinyl POSS (**POSS-vinyl**) (Scheme 1).

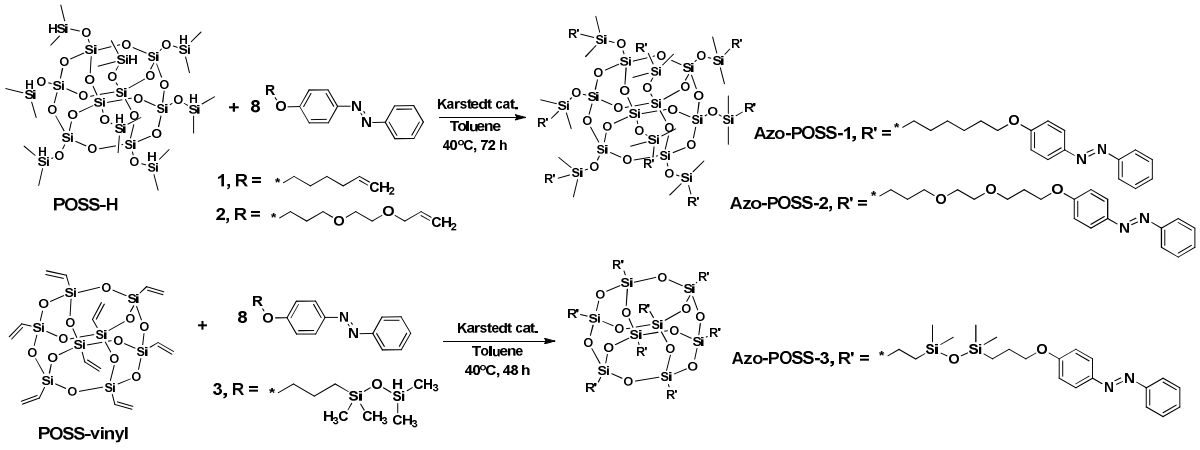

Scheme 1. Synthetic pathways for the synthesis of **Azo-POSS-1 – Azo-POSS-3**.

Compounds **Azo-POSS-4** and **Azo-POSS-5** were prepared by direct hydrosilylation reaction between **POSS-H** and allyl-functionalized azo dyes **4** (namely, the trimethylsilyl-protected dye **4**) and **5** bearing isolation groups respectively (Scheme 2). Note, protection of the hydroxyl groups of dye **4** is essential because they can easily react with Si-H bonds (*O*-silylation) [56, 57]. In order to prepare **Azo-POSS-4,** we synthesized trimethylsilyl-protected Azo-POSS compound (**Azo-POSS-4-TMS**) based on dye **4-TMS**. The trimethylsilyl protecting group was removed by stirring **Azo-POSS-4-TMS** at room temperature in methanol with acetic acid. Notably, that **Azo-POSS-4-TMS** molecule was easily hydrolyzed by moisture, even in air (see Figure SI4 for NMR data).

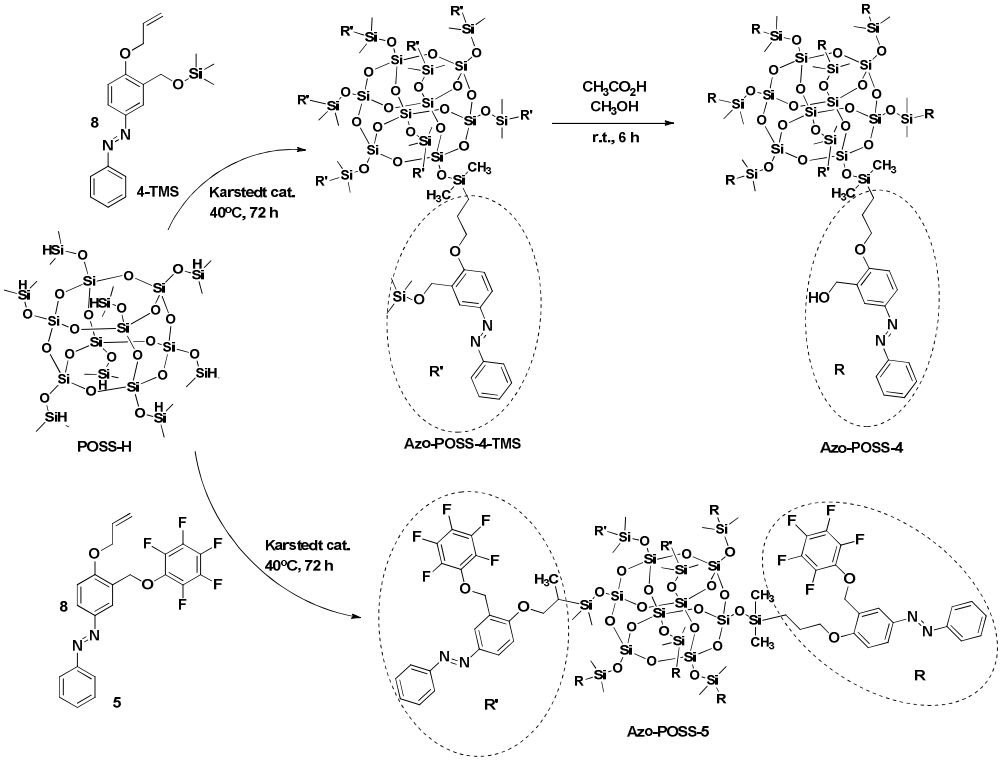

Scheme 2. Synthesis of **Azo-POSS-4** and **Azo-POSS-5**.

The hydrosilylation reaction was conducted by stirring initial POSS with 8 equiv of respective dye in dry toluene at 40 °C in the presence of platinum(0)-1,3-divinyl-1,1,3,3-tetramethyldisiloxane. The reactions were terminated after 72 h (for **Azo-POSS-1**, **Azo-POSS-2, Azo-POSS-4-TMS** and **Azo-POSS-5** based on **POSS-H**) or 48 h (for **Azo-POSS-3** based on **POSS-vinyl**). The completeness of the hydrosilylation reactions were confirmed by disappearance of characteristic proton multiplets due to Si-H or –CH=CH_2 bonds in the ^{1}H NMR spectra. Therefore, the mild reaction conditions were applied for all the synthesized Azo-POSS systems including the OH-functionalized Azo-POSS-4 preparation. Clearly, that the POSS cage configuration remained unchanged throughout the synthesis process. Thus, the inorganic POSS core shows significantly high thermal

and chemical stability and, importantly, is fully stable under relatively strong acidic conditions [58, 59].

The purification gave Azo-POSS conjugates in yields of 50−65 % as dark orange or brown powders which are soluble in toluene and chloroform. The structures of the synthesized Azo-POSS derivatives were characterized by ^{1}H, ^{13}C, ^{19}F NMR (in case of **Azo-POSS-5**), and FTIR spectrometry techniques, and were in good agreement with the proposed structures (Figure 2 and Figures SI1-SI6). Note that all POSS compounds except **Azo-POSS-5** are *β*-addition dominant products. According to the ^{1}H and ^{13}C NMR spectroscopic data, the **Azo-POSS-5** compound is a mixture resulting from both *α*- and *β*-addition. The abundance ratio of α- and β-isomers was estimated to be nearly 40%:60% from the integrals of isolated signals in the ^{1}H NMR spectrum. For **Azo-POSS-5** conjugate, the formation of a nearly equal amount of α- and β-addition products was observed most probably due to strong electron withdrawing characteristics of pentafluorophenyl group as well as steric constraints of the pentafluorophenoxymethylene group of dye **5** [60].

The successful installation of almost eight azobenzene moieties to the POSS core of the star-like molecules **Azo-POSS-1** and **Azo-POSS-3** was confirmed by ^{1}H NMR spectroscopy. The ^{1}H NMR spectroscopy indicated nearly complete modification of the octavalent POSS core of **Azo-POSS-2, Azo-POSS-4** and **Azo-POSS-5** molecules with azo dyes. From comparison of the integral areas of CH_3 proton signals of the POSS cage and the total integral area of attached dye molecules, the degree of functionalization can be obtained (see ^{1}H NMR spectra in SI). According to these calculations, the degree of functionalization was 87% for **Azo-POSS-2**, 83% for **Azo-POSS-4**, and 94% for **Azo-POSS-5**.

The successful grafting of azo dyes onto initial POSS scaffolds was additionally indicated by FTIR spectra (Figure 2). Generally, the Si-H characteristic absorption bands of **POSS-H** and dye **3** at around 2140 cm^{-1}, and vinyl characteristic absorption bands of **POSS-vinyl** and starting vinyl-based azo dyes at around 925 cm^{-1} disappeared in the FTIR spectra of the resulting Azo-POSS structures. Furthermore, the Azo-POSS molecules show characteristic C-H (in the region 3100-2800 cm^{-1}), aromatic C-C (at about 1600 and 1500 cm^{-1}), C-O-C (at around 1250 cm^{-1}) and Si-O-Si (at around 1100 cm^{-1}) stretching vibration. Note that the characteristic peak at 1142 due to Si-O-Si from the spacer was also found in the **Azo-POSS-3** spectrum, whereas the absorption bands at

1009 and 997 cm^{-1} in the FTIR spectrum of **Azo-POSS-5** indicate the presence of C-F groups.

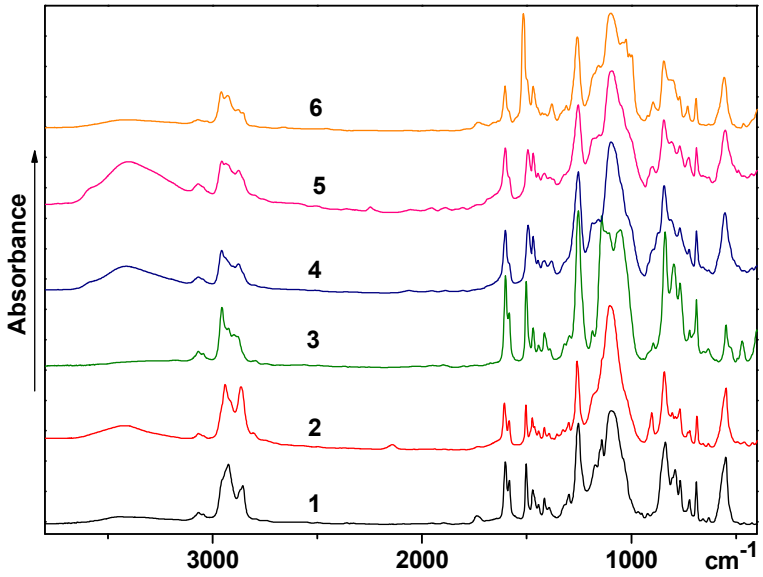

Figure 2. FTIR spectra of **Azo-POSS-1** (1), **Azo-POSS-2** (2), **Azo-POSS-3** (3), **Azo-POSS-4-TMS** (4), **Azo-POSS-4** (5) and **Azo-POSS-5** (6).

The electronic absorption spectra of the prepared azobenzene-modified POSS molecules in solution exhibit two characteristic absorption bands (Figure SI7). The high intensity band at 344–347 nm is related to $\pi-\pi^*$ transition of the *trans* form of the azobenzene moiety. The weak band in the range of 427–443 nm originates from typical $n-\pi^*$ transition. The absorbance peak positions ($\pi-\pi^*$ transition) of initial dye are identical to respective Azo-POSS compounds. However, the absorption bands corresponding to $\pi-\pi^*$ transition in the *trans* isomers of all Azo-POSS molecules are slightly broader compared to initial azo dyes. This broadening may be due to the partial chromophore-chromophore aggregation of the azobenzene fragments. Thus, the H- and J-aggregation of azobenzene normally will result in the blue and red shift of maximum absorption band [61]. Nevertheless, the absence of a pronounced shift of absorbance peak positions before and after dye conjugation to the POSS core indicates that in dilute solution aggregation is insignificant.

The spacer lengths (when fully extended) between a Si atom of the inorganic POSS core and a benzene ring of the azobenzene fragments in the resulted Azo-POSS were calculated from molecular models. In similar way, we recalculated the length of spacers for **Azo-POSS-long** and **Azo-POSS-short** conjugates which were synthesized by our research groups previously [43]. In that case, the spacer lengths of **Azo-POSS-long** and

Azo-POSS-short were estimated between a dimethylsilyl unit of the POSS core and a benzene ring of the corresponding dyes. Therefore, the branched POSS samples have spacers with following length: ~1.31 nm for **Azo-POSS-1**, ~1.78 nm for **Azo-POSS-2**, ~1.37 nm for **Azo-POSS-3,** ~0.95 nm for **Azo-POSS-4, Azo-POSS-5** and **Azo-POSS-short,** and ~2.16 nm for **Azo-POSS-long**.

Thermal (DSC) properties of azo dyes and Azo-POSS conjugates. Thermal properties of initial dyes **1**-**5** and substituted oligomeric silsesquioxanes **POSS-Azo-1 - POSS-Azo-5** were investigated using differential scanning calorimetry (DSC) (Figures 3a and 3b). The DSC was performed in a temperature range of −50 to 150 °C with heating and cooling rates of 10 °C/min. The melting temperature (T_m) and enthalpy ($_{\Delta}H_m$) of azo dyes was determined from the first heating cycle, and the second heating run was used to determine the glass transition (T_g) and the melting characteristics of Azo-POSS conjugates. The DSC thermograms of initial azo dyes exhibit a single endothermic peak due to the melting (Figure 3a). Dyes **1**, **3**, **4** and **5** showed T_m values of 45, 32, 57 and 67 ^{o}C respectively. The $_{\Delta}H_m$ values were determined to be 101 J/g for dye **1**, 56 J/g for dye **3**, 112 J/g for dye **4** and 82 J/g for dye **5** (Fig. SI8). No melting endothermic peak was found from the DSC curve for azo dye **2**.

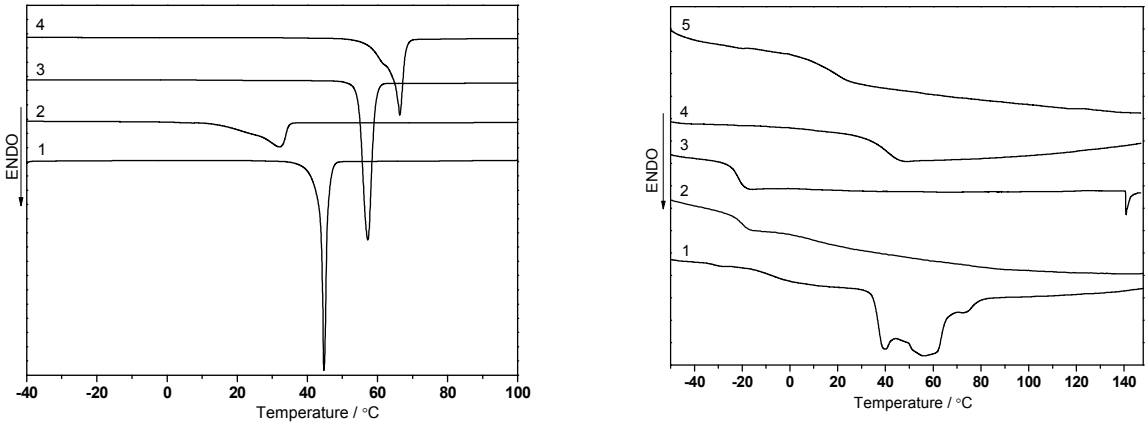

a **b**

Figure 3. (a) DSC data of azo dyes **1** (1), **3** (2), **4** (3) and **5** (4). (b) DSC data of **Azo-POSS-1** (1), **Azo-POSS-2** (2), **Azo-POSS-3** (3), **Azo-POSS-4** (4) and **Azo-POSS-5** (5). DSC curves are offset for clarity.

As determined from the inflection point position on the DSC curve, Azo-POSS-1 has a T_g of -9 °C. Further, the multiple crystallization peaks (up to three) come from different crystal modifications were observed on the DSC thermogram of the **Azo-POSS-1** compound (Figure 3b and Table 1). Note that the whole melting enthalpy of **Azo-POSS-1** system is 23 J/g that is significantly lower in comparison to initial dye **1**. In contrast, compounds **Azo-**

POSS-2 − Azo-POSS-5 only showed glass transitions at -21, -22, 37 and 15 °C, respectively (Figure 3b and Table 1). The glass transition range (ΔT_g) of the synthesized Azo-POSS compounds are presented in Table 1.

Table 1 Thermal properties of Azo-POSS compounds.

Sample	T_m, (°C)	T_g, (°C)	ΔT_g, (°C)
Azo-POSS-1	40; 56, 73	-9	20
Azo-POSS-2	-	-21	7
Azo-POSS-3	141	-22	7
Azo-POSS-4	-	37	18
Azo-POSS-5	-	15	18

T_m – melting point, T_g – glass transition temperatures, ΔT_g – glass transition range.

It should be noted that the DSC thermogram of **Azo-POSS-3** have an additional small exothermic peak above the glass transition temperature in the high temperature region (141 °C). This peak can be attributed to a presence of a LC phase and are related to the melting (crystal-liquid) transition. The first DSC heating run of **Azo-POSS-3** derivative did not reveal any melting endothermic peak.

It is known that the original **POSS-H** and **POSS-vinyl** compounds are highly crystalline materials and have many sharp diffraction peaks on X-ray diffraction (XRD) patterns [62-64]. Examples of wide angle XRD patterns are illustrated in Figure SI9 to provide further information about crystal structure of **Azo-POSS-1** and **Azo-POSS-3** samples. One can see that **Azo-POSS-3** shows two diffusion peaks at $2\theta = 6.2^o$ and $2\theta = 15.0^o$ which indicate amorphous nature of this sample. At the same time, for **Azo-POSS-1**, two characteristic dominant diffraction peaks at $2\theta = 6.0^o$ and $2\theta = 19.2^o$ also were found. However, the latter peaks increased in intensity and sharpness. From this observation, it was confirmed that the **Azo-POSS-1** conjugate formed the crystalline domains. These results are in agreement with the data from DSC analysis. Hence, according to DSC and XRD data the introduction of the isolation groups to the chromophore moieties as well as sufficiently long spacer between the inorganic core and the azobenzene moiety is an efficient approach to minimize the crystallinity of the materials and thus to facilitate formation of uniform amorphous films with low scattering. It is reasonable to suggest that conjugation of crystallized molecular organic compound with the bulky POSS cages has resulted in amorphous hybrid materials due to disruption of the packing. This effect is well-documented [32, 33, 40, 42, 62, 63, 65, 66].

Thin films prepared from Azo-POSS conjugates. Our previous results demonstrated that all starting azo dyes gave discontinuous and inhomogeneous films due

to crystallization and aggregation [54]. One might expect the covalent linkage of the dyes to the POSS molecules will facilitate the formation of uniform ultrathin films. Therefore, we investigated the formation of thin films from the synthesized Azo-POSS conjugates by spin-coating toluene solution (20 mg/mL) onto quartz substrates. It has been found that it is possible to obtain stable ultrathin films from Azo-POSS compounds. The UV-vis absorption spectra of Azo-POSS films (Figure 4) closely resembled solution spectra. Nevertheless, the UV-vis adsorption band for **Azo-POSS-4** is slightly broadened and bathochromically shifted compared to other Azo-POSS conjugates. The fact that the difference between them is that Azo-POSS-4 contains OH group in the azobenzene moiety. The hydroxyl-functionalized compounds are widely used in supramolecular chemistry for the construction of hydrogen-bonded assemblies [67]. Thus, observation of broadening of adsorption band in **Azo-POSS-4** spectrum indicates that intermolecular interactions between its azochromophores take place.

Thickness (*d*) of the resulting films was estimated using spectroscopic ellipsometry (SE) to be 61.8, 55.4, 62.0, 54.5 and 58.9 nm for **Azo-POSS-1**, **Azo-POSS-2**, **Azo-POSS-3**, **Azo-POSS-4** and **Azo-POSS-5** respectively.

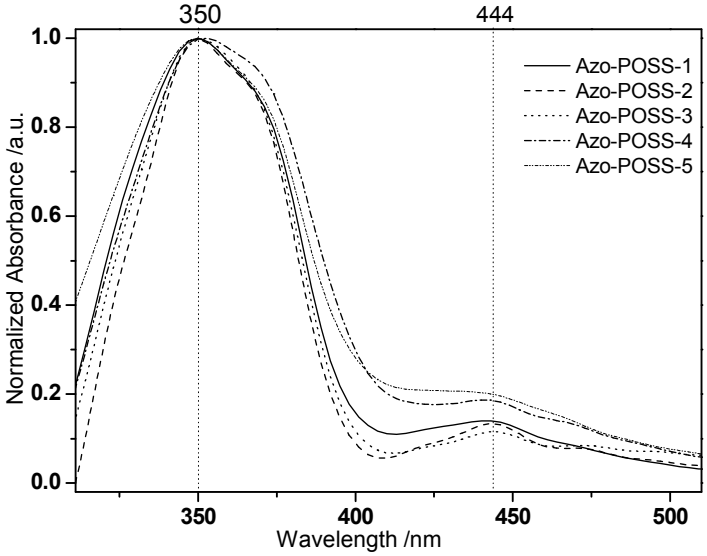

Figure 4. UV-vis absorbance spectra of Azo-POSS thin films

AFM analysis of surface morphology of films based on the Azo-POSS conjugates shows that morphology of films and their roughness (Rq) can be tuned by variation of spacer type between the azobenzene and POSS core (Figure 5). **Azo-POSS-1** compound (lengths of spacer is 1.31 nm) formed a film with developed crystalline domains (average height of crystalline domains is about 60 nm and average area per domain is about 150 μm^2).

Surface roughness of film from **Azo-POSS-1** is 23.9 nm with surface area 30 x 30 μm (Figure 5a and b). Surface roughness decreasing from 23.9 nm (sample **Azo-POSS-1**) to 2.6 nm (sample **Azo-POSS-3**; for **Azo-POSS-2** – 8.1 nm) with increasing length of the spacer between the azobenzene and POSS core (Figures 5b and c). From our previous study [42] and, according to current DSC and AFM data, we can conclude that the length of flexible spacers for formation of amorphous Azo-POSS film with smooth surface should be longer than 0.95 nm. On the other hand, it appears that the insertion of organic-inorganic spacer (~1.37 nm) into the Azo-POSS system has a positive effect on the film-forming properties of azo-based POSS conjugates. At the same time, Azo-POSS derivatives with isolation groups exhibit formation of smooth films with the lowest roughness of 1.49 nm for **Azo-POSS-4** and 1.1 nm for **Azo-POSS-5** (Figures 5d and e).

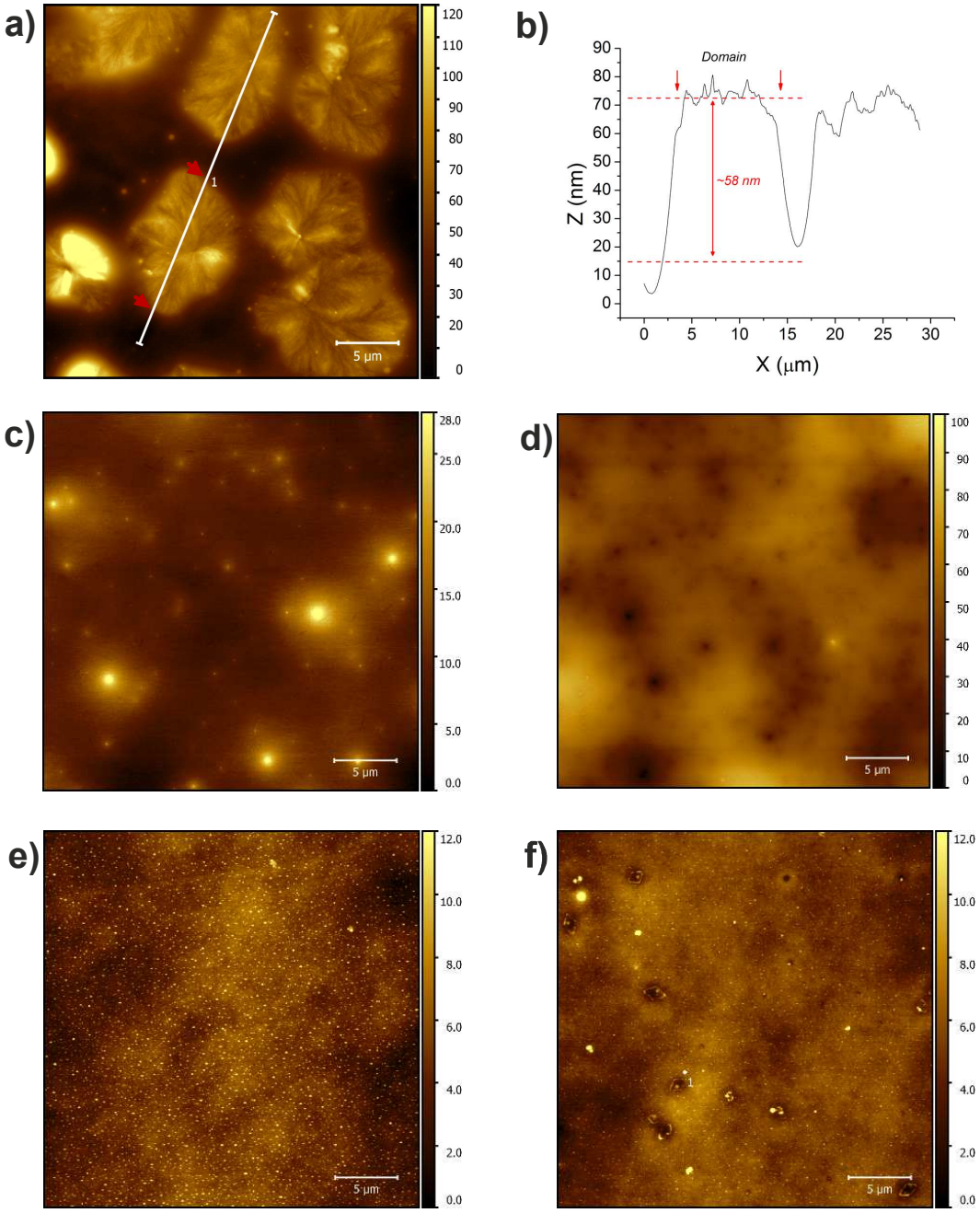

Figure 5. AFM topographical images of films based on different Azo-POSS compounds: **Azo-POSS-1** (a) and cross-section profile along white line (b), **Azo-POSS-2** (c), **Azo-POSS-3** (d), **Azo-POSS-4** (e) and **Azo-POSS-5** (f).

POSS doping is used extensively to improve the optical properties of materials due to the low refractive index and scattering of oligomeric silsesquioxanes [68]. The ability of the synthesized Azo-POSS derivatives to form ultrathin films makes it possible to accurately determine the refractive indexes of these compounds. Thus, the real refractive index (*n*) values of all Azo-POSS can be extracted from SE measurements [42]. The *n* values for **Azo-POSS-1**, **Azo-POSS-2**, **Azo-POSS-3**, **Azo-POSS-4** and **Azo-POSS-5** at the

absorption maxima (λ_{max}) are 1.466, 1.470, 1.464, 1.478 and 1.456 respectively. Fluorine-containing compound Azo-POSS-5 showed the lowest real refractive index according to SE. It is well known that the substitution of hydrogen with fluorine is regarded as being a good way to reduce the refractive index of compounds [69, 70]. Generally, refractive indices for all Azo-POSS systems are comparable or even lower with traditional low refractive index materials based on azobenzenes and polycarbonates or polyacrylates [42]. The dielectric constant ε can be also determined based on the ellipsometry data as the squared refractive index at zero frequency, n_1. Assuming Lorentz function for weakly interacting oscillators (chromophores), one can consider $n_1 \approx n(\lambda_{max})$ (i.e., at the wavelength of the absorption maximum) and therefore $\varepsilon \approx n^2(\lambda_{max})$ [53]. Therefore, all Azo-POSS derivatives showed low dielectric constant with the values ε in the range of 2.12-2.18.

Photoisomerization of Azo-POSS molecules in solution and thin film. Well-known fact that azobenzenes can undergo a rapid *trans-cis* photoisomerization when the π-π^* transition is excited. The back isomerization occurs in the dark with rate depend on the structure of azo-based compounds [7]. Relatively slow kinetics and distinct UV-vis profiles of the *trans* and *cis* form of monoazobenzene allow monitoring the conversion with a simple spectrophotometric setup [42]. Indeed, typical photoisomerization behavior was observed for all initial dyes **1-5** in solution [54]. These results indicated that the length of alkyl tails (dye **1-3**) has no significant effect on the photoisomerization, whereas introduction of the side isolation substituents in the *ortho*-position to the ether linkage of the azobenzene fragment of the dyes **4** and **5** provided a decreasing of photoisomerization rate constants (Table 2). It was suggested that the reduced rate of photoisomerization of azo-based chromophores with isolation groups may be attributed to the change of the electronic nature of azobenzene fragment.

Table 2. The values of photoisomerization rate constants of dye **1-5** and Azo-POSS compounds (in solution and film state)

Azo dye	Rate constant of photoisomerization, (s^{-1})	Azo-POSS	Rate constant of photoisomerization, (s^{-1})	
	solution		solution	film
1	0.131	**Azo-POSS-1**	0.113	0.0132
2	0.118	**Azo-POSS-2**	0.102	0.0122
3	0.126	**Azo-POSS-3**	0.100	0.0131
4	0.055	**Azo-POSS-4**	0.069	0.0113
5	0.058	**Azo-POSS-5**	0.070	0.0099

In order to achieve photoisomerization of the synthesized Azo-POSS systems (**Azo-POSS-1** – **Azo-POSS-5**) respective 0.005 mg/mL solutions in chloroform were irradiated with 365 nm UV-light. The first-order rate constant of photoisomerization can be determined from the slope of the plot of $\ln[(A_0 - A_\infty)/(A_t - A_\infty)]$ vs time where A_0, A_∞, and A_t are the absorbances before irradiation, after reaching a photostationary state, and at a given time, respectively [42]. The photoisomerization experiments were performed in triplicate for each sample, and the averaged data points along with linear fits are presented in Figure 6.

It was found that depending the chemical structures of Azo-POSS conjugates, the photoisomerization reached a photostationary state after UV irradiation for 50-70 s (Figure 6).

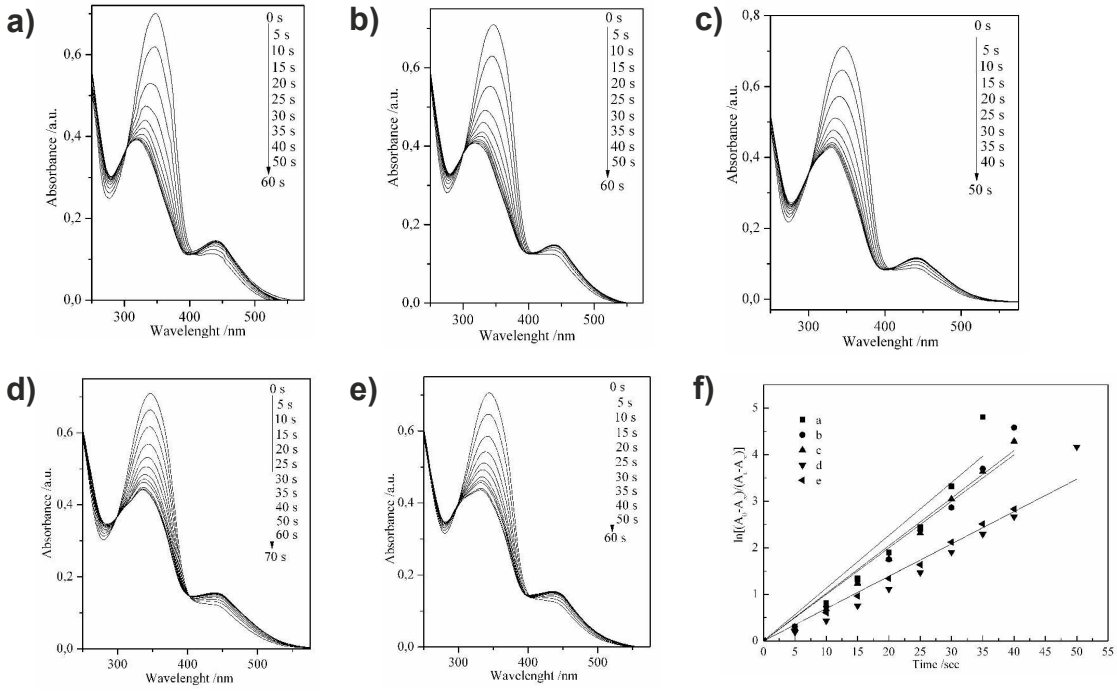

Figure 6. UV-vis spectra of compounds (a) **Azo-POSS-1**, (b) **Azo-POSS-2**, (c) **Azo-POSS-3**, (d) **Azo-POSS-4** and (e) **Azo-POSS-5** under UV irradiation at 365 nm. (d) Kinetics of the *cis-trans* isomerization of **Azo-POSS-1** (line a), **Azo-POSS-2** (line b), **Azo-POSS-3** (line c), **Azo-POSS-4** (line d) and **Azo-POSS-5** (line e) in $CHCl_3$ solution.

A series of derivatives **Azo-POSS-1**, **Azo-POSS-2** and **Azo-POSS-3** with different spacer lengths and chemical nature between the inorganic POSS core and the azobenzene moiety had almost similar photoisomerization rate constants. As in the case of the initial dyes **1-5**, the photoisomerization rates of **Azo-POSS-4** and **Azo-POSS-5** based on azobenzenes with lateral substituents of the azobenzene fragment were

relatively slower compared to **Azo-POSS-1** - **Azo-POSS-3** compounds (Table 2 and Figure 6).

It is important to note, according to the first-order rate constant of *trans*-*cis* photoisomerization, the photoisomerization for **Azo-POSS-1**, **Azo-POSS-2** and **Azo-POSS-3** is decreased by a factor of approximately 1.2 compared with the corresponding dyes **1**, **2** and **3**. Surprisingly, the introduction of isolation groups to the chromophore moieties of **Azo-POSS-4** and **Azo-POSS-5** conjugates resulted in ~1.2 times faster the photoisomerization rate comparatively with the respective azo dyes **4** and **5** (Table 2). These results indicate that, within one molecule, partial aggregation of azobenezene fragments occurs in **Azo-POSS-1** – **Azo-POSS-3** compounds whereas the insertion of isolation hydroxymethylene- and pentafluorophenoxymethylene-groups into **Azo-POSS-4** and **Azo-POSS-5** conjugates is powerful to prevent intramolecular aggregation of their azobenzene chromophores.

It should be noted that the photoisomerization has not been observed in the star-shaped azobenzene-modified Azo-POSS with long oxyhexyl-oxyethoxy-propyl spacer between the core and the azobenzene fragments (2.16 nm) in film state due to the aggregation of azo dyes. It was suggested that the flexible long spacer allows free movement and rotation of the azobenzene fragments which lead to their aggregation, and, consequently, such azobenzene units do not normally undergo photoisomerization [40]. Importantly, the thin films of the obtained Azo-POSS systems exhibited a pronounced change in intensity of the $\pi-\pi^*$ transition at 350 nm, indicating efficient *trans*-to-*cis* isomerization (Figure 7).

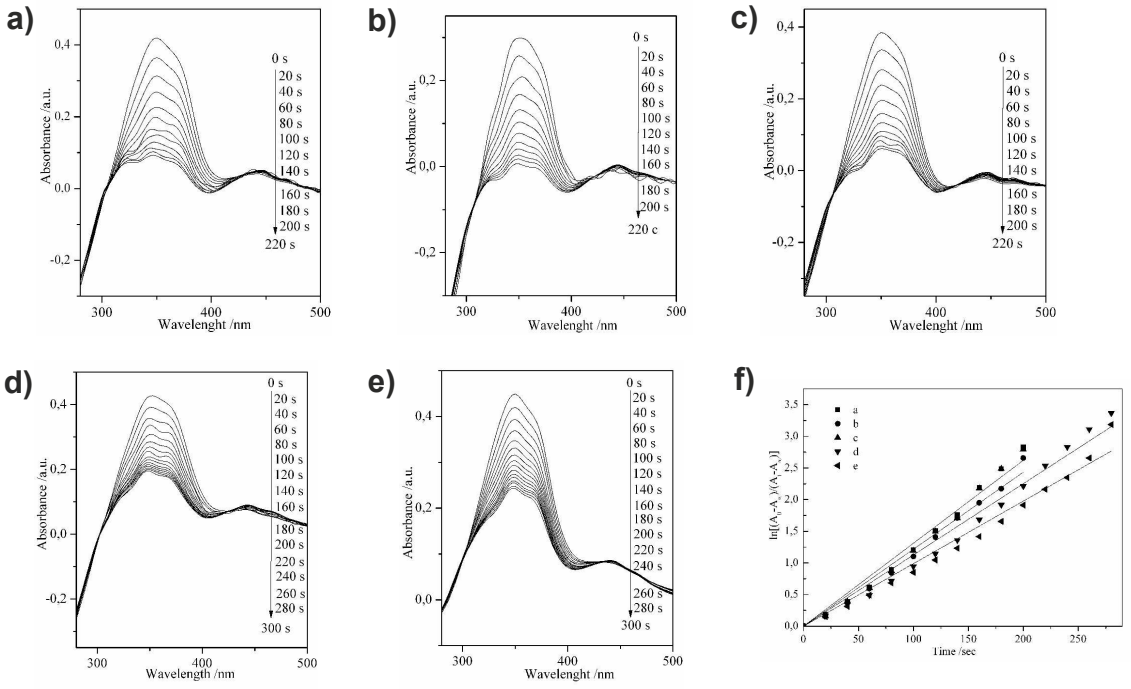

Figure 7. UV-vis spectra of the films (a) **Azo-POSS-1**, (b) **Azo-POSS-2**, (c) **Azo-POSS-3**, (d) **Azo-POSS-4** and (e) **Azo-POSS-5** under UV irradiation at 365 nm. (d) Kinetics of the *cis-trans* isomerization of **Azo-POSS-1** (line a), **Azo-POSS-2** (line b), **Azo-POSS-3** (line c), **Azo-POSS-4** (line d) and **Azo-POSS-5** (line e) in film.

In that way it is clear that for the synthesis of branched azobenzene-modified POSS samples that are able to form uniform, ultrathin films, and undergo light induced isomerization, the spacer length of initials dyes should be regulated in the range 1.2 to 1.9 nm.

The photoisomerization of Azo-POSS compounds in thin films was slower than in solution with a significant portion of *trans* isomer present even after 3 min of UV irradiation as expected from literature [42]. Precise analysis of the obtained data provide the evidence of high effectiveness of side isolation groups to prevent both inter- and intramolecular aggregation of the azobenzenene units. Thus, the rates of *trans*-to-*cis* photoisomerization of **Azo-POSS-1** – **Azo-POSS-3** compounds in thin films were about 8 times slower than that in solutions. In contrast, the values of photoisomerization rate constants of **Azo-POSS-4** and **Azo-POSS-5** with lateral substituents in the *ortho* position to the ether linkage of the azobenzene fragment were less than 8 times (in 6 times for **Azo-POSS-4** and in 7 times for **Azo-POSS-5**) slower than that in solutions (Table 2). Hence, some interesting trends were observed: (i) the rates of photoisomerization of the initial chromophores without the isolation group (**1**, **2** and **3**) in solutions are faster more

than 2 times than the *trans-cis* isomerization rates observed for dyes with isolation groups; (ii) the photoisomerization rates of **Azo-POSS** systems without the isolation group in the azobenzene fragment (**Azo-POSS-1**, **Azo-POSS-2** and **Azo-POSS-3**) in solutions are faster about 1.6 times than the *trans-cis* isomerization rates observed for **Azo-POSS-4** and **Azo-POSS-5** molecules with isolation groups in azobenzene unit; and (iii) the photoisomerization rates of **Azo-POSS-1**, **Azo-POSS-2** and **Azo-POSS-3** in thin films are only slightly faster (~ 1.3 times) than the *trans-cis* isomerization rates found in thin films of **Azo-POSS-4** and **Azo-POSS-5.**

A simple calculation (taking into account that we have the structures of octasubstituted Azo-POSS compounds) shows that the molar content of azobenzenes units (namely diphenyldiazene units, M = 182.2 g/mol) of Azo-POSS-1, Azo-POSS-2, Azo-POSS-3, Azo-POSS-4 and Azo-POSS-5 is 46.2%, 44.4%, 41.7%, 47.6% and 33.5. Thus, the amount of chromophores content has tended to remain about the same with exception of the Azo-POSS-5. Of particular importance is the finding that despite the significant differences in content of azobenzene units between Azo-POSS-4 with a maximum amount of azobenzenes and Azo-POSS-5 with a minimum amount of azobenzenes (both have isolations groups in azobenzene fragments), we found their photoisomerization behaviors (either in solution or film) were remarkably similar. It means that photoisomerization behaviors of the synthesized Azo-POSS molecules are mainly depends on their chemical structures, and not on the azobenzene content. However, the chemical nature of isolation groups (similar to the length and structure of spacers) affect on thermal, film-forming and optical (dielectric) properties of the studied systems.

Overall, all branched POSS compounds synthesized here show the photoisomerization behavior both in solvent and solid film. The conjugation of azobenzenes with isolation moieties to the POSS-based scaffold resulted in diverse *trans-cis* isomerization behavior (namely, the rates of photoisomerization) compared with branched Azo-POSS structures possessing only flexible spacers between the inorganic POSS core and the active azobenzene units. The obtained results indicate that the side groups afford more stable isomerazation behavior of Azo-POSS compounds by preventing aggregation of azobenzene chromophores. In fact it is well known the site-isolation principle is very useful for the rational design of new polymers with effective nonlinear optic characteristics [55], but such concept has not been applied in detail to reversible photoisomerization systems based on branched Azo-POSS structures.

Conclusions

In conclusion, we synthesized a new series of branched Azo-POSS structures possessing flexible spacers of different chemical natures and lengths between the inorganic POSS core and the azobenzene branches. Additionally, for the first time to our knowledge, we developed synthetic route for new Azo-POSS systems with changeable isolation groups (hydroxymethylene- and pentafluorophenoxymethylene moieties) in the azobenzene fragments and the constant short spacer between azo dyes and medium. The benefits of the proposed Azo-POSS structures are their ability to facilitate formation of uniform amorphous (with exception of Azo-POSS-1 sample) films in which photoisomerization occurs. At the same time, star-shaped Azo-POSS conjugates based on monoazobenzene derivatives, which were previously synthesized by our research groups, could either form the uniform amorphous films without the ability to azobenzene photoisomerization (Azo-POSS-long) or form a relatively rough films with the ability to azobenzene photoisomerization (Azo-POSS-short) in such solid films [42, 43]. It is important underline that approach connected with synthesis of Azo-POSS conjugates based on azobenezenes having side isolation groups is the most useful to fabricate uniform and amorphous films with a decreased microroughness and, more importantly, to prevent inter- and intramolecular aggregation of azobenzene chromophores attached to POSS core in solid state. We suggest that the photoisomerization of Azo-POSS films with isolation groups in azobenzene unit will be more stable over the long term owing the ability of isolation groups effectively to prevent azo dye aggregation. Furthermore, in this and previous reports [42, 43] we have demonstrated that control of the distance between the azobenzene unit and the POSS core, and variation of the chemical natures of the spacers are also the critical conditions for the formation of the Azo-POSS films with a uniform and smooth morphology and photoisomerization ability of azobenzene fragments in such films. Thus, the obtained Azo-POSS structures with high dye grafting density, suppressed crystallization and low optical losses could be promising candidates for practical application in the robust photoresponsive coatings.

Conflicts of interest

There are no conflicts to declare.

Acknowledgments

The research at Georgia Tech (Dr. Volodymyr Korolovych and Prof. Vladimir Tsukruk) is supported by the NSF DMR 1505234 project (morphology study) and the U.S.

Department of Energy, Office of Basic Energy Sciences, Division of Materials Sciences and Engineering under Award # DE-FG02-09ER46604 (photooptical properties) .

References

1. H.D. Bandara and S.C. Burdette, *Chem. Soc. Rev.,* 2012, **41**, 1809-1825.
2. A. Díaz-Moscoso and P. Ballester, *Chem. Commun*., 2017, **53**, 4635-4652.
3. S. Erbas-Cakmak, D.A. Leigh, C.T. McTernan and A.L. Nussbaumer, *Chem. Rev.,* 2015, **115**, 10081-10206.
4. E. Merino, *Chem. Soc. Rev.,* 2011, **40**, 3835-3853.
5. E. Merino and M. Ribagorda, *Beilstein J. Org. Chem.,* 2012, **8**, 1071-1091.
6. F.P. Nicoletta, D. Cupelli, P. Formoso, G. De Filpo, V. Colella and A. Gugliuzza, *Membranes,* 2012, **2**, 134-197.
7. Z. Mahimwalla, K.G. Yager, J.I. Mamiya, A. Shishido, A. Priimagi and C.J. Barrett, *Polym. Bull.,* 2012, **69**, 967-1006.
8. J. Plain, G.P. Wiederrecht, S.K. Gray, P. Royer and R. Bachelot, *J. Phys. Chem. Lett.,* 2013, **4**, 2124-2132.
9. K.L. Genson, J. Holzmuller, O.F. Villacencio, D.V. McGrath, D. Vaknin and V.V. Tsukruk, *J. Phys. Chem. B*., 2005, **109**, 20393-20402.
10. A. Adam and G. Haberhauer, *J. Am. Chem. Soc*., 2017, **139**, 9708-9713.
11. C.Y. Lai, G. Raj, I. Liepuoniute, M. Chiesa and P. Naumov, *Cryst. Growth Des.,* 2017, **17**, 3306-3312.
12. C. Li, J.H. Yun, H. Kim and M. Cho, *Macromolecules,* 2016, **49**, 6012-6020.
13. C. Kouvatas, W.E. Baille, J. Ortíz-Palacios, E. Aguilar-Ortíz, E. Rivera and X.X. Zhu, *J. Phys. Chem. B*., 2015, **119**, 12318-12324.
14. E.N. Cho, D. Zhitomirsky, G.G. Han, Y. Liu and J.C. Grossman, *ACS Appl. Mater. Interfaces,* 2017, **9**, 8679-8687.
15. Z.X. Liu, Y. Feng, Z.C. Yan, Y.M. He, C.Y. Liu and Q.H. Fan, *Chem. Mater.,* 2012, **24**, 3751-3757.
16. K.L. Genson, D. Vaknin, O. Villacencio, D.V. McGrath and V.V. Tsukruk, *J. Phys. Chem. B.,* 2002, **106**, 11277-11284.
17. O. Nachtigall, R. Lomoth, C. Dahlstrand, A. Lundstedt, A. Gogoll, M.J.. Webb and H. Grennberg, *Eur. J. Org. Chem.,* 2014, **2014**, 966-972.
18. H. Umezawa, M. Jackson, O. Lebel, J.M. Nunzi and R.G. Sabat, *Opt. Mater.,* 2016, **60**, 258-263.
19. A. Bobrovsky, N. Boiko and V. Shibaev, *Polymer,* 2015, **56**, 263-270.

20. A. Sidorenko, C. Houphouet-Boigny, O. Villavicencio, M. Hashemzadeh, D.V. McGrath and V.V. Tsukruk, *Langmuir,* 2000, **16**, 10569-10572.

21. S. Guo, J. Sasaki, S. Tsujiuchi, S. Hara, H. Wada, K. Kuroda and A. Shimojima, *Chem. Lett.,* 2017, **46**, 1237-1239.

22. A. Ziegler, J. Stumpe, A. Toutianoush and B. Tieke, *Colloids Surf. A.,* 2002, **198**, 777-784.

23. T. Chen, S. Xu, F. Zhang, D.G. Evans and X .Duan, *Chem. Eng. Sci.,* 2009, **64**, 4350-4357.

24. T. Sato, Y. Ozaki and K. Iriyama, *Langmuir*, 1994, **10**, 2363-2369.

25. W. Wu, C. Ye, J. Qin and Z. Li, *Polymer*, 2012, **53**, 153-160.

26. S. Guo, T. Okubo, K. Kuroda and A. Shimojima, *J. Sol-Gel Sci. Technol.,* 2016, **79**, 262-269.

27. H. Chi, K.Y. Mya, T. Lin, C. He, F. Wang and W.S. Chin, *New J. Chem.,* 2013, **37**, 735-742.

28. F. Ke, S. Wang, S. Guang, Q. Liu and H. Xu, *Dyes Pigm.,* 2015, **121**, 199-203.

29. C. Hartmann-Thompson, D.L. Keeley, K.M. Pollock, P.R. Dvornic, S.E. Keinath, M. Dantus, T.C. Gunaratne and D.J. LeCaptain, *Chem. Mater.,* 2008, **20**, 2829-2838.

30. D. Clarke, S. Mathew, J. Matisons, G. Simon and B.W. Skelton, *Dyes Pigm.,* 2012, **92**, 659-667.

31. E. Lucenti, C. Botta, E. Cariati, S.Righetto, M. Scarpellini, E. Tordin and R. Ugo, *Dyes Pigm.,* 2013, **96**, 748-755.

32. Y. Xiao, L. Liu, C. He, W.S. Chin, T. Lin, K.Y. Mya, J. Huang and X. Lu, *J. Mater. Chem.,* 2006, **16**, 829-836.

33. M.Y. Lo, C. Zhen, M. Lauters, G.E. Jabbour and A. Sellinger, *J. Am. Chem. Soc.,* 2007, **129**, 5808-5809.

34. J. Zhou, Y. Zhao, K. Yu, X. Zhou and X. Xie, *New J. Chem.* 2011, **35**, 2781-2792.

35. N.R. Vautravers, P. André, A.M.Z. Slawin and D.J. Cole-Hamilton, *Org. Biomol. Chem.,* 2009, **7**, 717-724.

36. J.D. Froehlich, R. Young, T. Nakamura, Y. Ohmori, S. Li, A. Mochizuki, M. Lauters and G.E. Jabbour, *Chem. Mater.,* 2007, **19**, 4991-4997.

37. A. Miniewicz, M. Tomkowicz, P. Karpinski, L. Sznitko, B. Mossety-Leszczak and M. Dutkiewicz, *Chem. Phys.,* 2015, **456**, 65-72.

38. A. Miniewicz, J. Girones, P. Karpinski, B. Mossety-Leszczak, H. Galina and M. Dutkiewicz, *J. Mater. Chem. C*., 2014, **2**, 432-440.

39. X. Su, H. Xu, Y. Deng, J. Li, W. Zhang and P. Wang, *Mater. Lett.,* 2008, **62**, 3818-3820.

40. Y. Liu, W. Yang and H. Liu, *Chem. Eur. J.,* 2015, **21**, 4731-4738.

41. X. Su, S. Guang, H. Xu, X. Liu, S. Li, X. Wang, Y. Deng and P. Wang, *Macromolecules,* 2009, **42**, 8969-8976.

42. P.A. Ledin, I.M. Tkachenko, W. Xu, I. Choi, V.V. Shevchenko and V.V. Tsukruk, *Langmuir,* 2014, **30**, 8856-8865.

43. P.A. Ledin, M. Russell, J.A. Geldmeier, I.M. Tkachenko, M.A. Mahmoud, V. Shevchenko, M.A. El-Sayed and V.V. Tsukruk, *ACS Appl. Mater. Interfaces,* 2015, **7**, 4902-4912.

44. Y. Zhang, L. Zhang, H. Liu, D. Sun and X. Li, *Cryst. Eng. Comm.,* 2015, **17**, 1453-1463.

45. Y. Diao, L. Shaw, Z. Bao and S.C. Mannsfeld, *Energy Environ. Sci.,* 2014, **7**, 2145-2159.

46. L. Song, X. Cao, L. Li, Q. Wang, H. Ye, L. Gu, C. Mao, J. Song, S. Zhang and H. Niu, *Adv. Funct. Mater.,* 2017, **27**, 1700474.

47. R.C. Tenent, T.M. Barnes, J.D. Bergeson, A.J. Ferguson, B. To, L.M. Gedvilas, M.J. Heben and J.L. Blackburn, *Adv. Mater.,* 2009, **21**, 3210-3216.

48. V.V. Shevchenko, A.V. Sidorenko, V.N. Bliznyuk, I.M. Tkachenko and O.V. Shekera, *Polym. Sci. Ser. A*., 2013, **55**, 1-31.

49. Z.A. Li, W. Wu, C. Ye, J. Qin and Z. Li, *J. Phys. Chem. B*., 2009, **113**, 14943-14949.

50. Z.A. Li, Q. Zeng, G. Yu, Z. Li, C. Ye, Y. Liu and J. Qin, *Macromol. Rapid Commun.,* 2008, **29**, 136-141.

51. W. Wu, Q. Huang, C. Zhong, C. Ye, J. Qin and Z. Li, *Polymer*, 2013, **54**, 5655-5664.

52. V.V. Shevchenko, A.V. Sidorenko, V.N. Bliznyuk, I.M. Tkachenko, O.V. Shekera, N.N. Smirnov, I.A. Maslyanitsyn, V.D. Shigorin, A.V. Yakimansky and V.V. Tsukruk, *Polymer,* 2013, **54**, 6516-6525.

53. R. Tang and Z. Li, *Chem. Rec.*, 2017, **17**, 71-89.

54. I.M. Tkachenko, Y.L. Kobzar, O.G. Purikova, A.L. Tolstov, O.V. Shekera and V.V. Shevchenko, *Tetrahedron Lett*., 2016, **57**, 5505-5510.

55. Z. Li, Q. Li and J. Qin, *Polym. Chem.,* 2011, **2**, 2723-2740.

56. C. Zhang and R.M. Laine, *J. Am. Chem. Soc.,* 2000, **122**, 6979-6988.

57. A.A. Pakhomov, Y.N. Kononevich, M.V. Stukalova, E.A. Svidchenko, N.M. Surin, G.V. Cherkaev, O.I. Shchegolikhina, V.I. Martynov and A.M. Muzafarov, *Tetrahedron Lett., 2016,* **57**, 979-982.

58. S. Wang, L. Tan, C. Zhang, I. Hussain and B. Tan, *J. Mater. Chem. A*, 2015, **3**, 6542-6548.

59. K. Tanaka and Y. Chujo, *J. Mater. Chem.,* 2012, ***22***, 1733-1746.

60. X. Wang, Q. Ye, J. Song, C.M. Cho, C. He and J. Xu, *RSC Adv.,* 2015, **5**, 4547-4553.

61. W. Zhang, J. Xie, W. Shi, X. Deng, Z. Cao and Q. Shen, *Eur. Polym. J.,* 2008, **44**, 872-880.

62. C.C. Cheng, C.H. Chien, Y.C. Yen, Y.S. Ye, F.H. Ko, C.H. Lin and F.C. Chang, *Acta Mater.*, 2009, **57**, 1938-1946.

63. M. Ariraman and M. Alagar, *Rsc Adv.,* 2014, **4**, 19127-19136.

64. D. Chen, S. Yi, W. Wu, Y. Zhong, J. Liao, C. Huang and W. Shi, *Polymer,* 2010, **51**, 3867-3878.

65. X. Su, S. Guang, H. Xu, J. Yang and Y. Song, *Dyes Pigm.,* 2010*,* **87**, 69-75.

66. F. Wang, X. Lu and C. He, *J. Mater. Chem.,* 2011, **21**, 2775-2782.

67. A. Ajayaghosh, S.J. George, A.P. Schenning, *Top. Curr. Chem.*, 2005, **258**, 83-118

68. R. Sastre, V. Martin, L. Garrido, J.L. Chiara, B. Trastoy, O. Garcia, A. Costela and I. Garcia-Moreno, *Adv. Funct. Mater.*, 2009, **19**, 3307-3316.

69. I.M. Tkachenko, N.A. Belov, Y.V. Yakovlev, P.V. Vakuliuk, O.V. Shekera, Y.P. Yampolskii and V.V. Shevchenko, *Mat. Chem. Phys.,* 2016*,* **183**, 279-287.

70. D. Shamiryan, T. Abell, F. Iacopi and K. Maex, *Mater. Today,* 2004, **7**, 34-39.

TOC

Novel Branched Nanostructures Based on Polyhedral Oligomeric Silsesquioxanes and Azobenzene Dyes Containing Different Spacers and Isolation Groups

Ihor M. Tkachenko,[a] Yaroslav L. Kobzar,[a] Volodymyr F. Korolovych,[b] Alexandr V. Stryutsky,[a] Liubov K. Matkovska,[a] Valery V. Shevchenko,*[a] Vladimir V. Tsukruk*[b]

[a] Institute of Macromolecular Chemistry, National Academy of Sciences of Ukraine, Kharkivske shosse 48, Kyiv, 02160, Ukraine

[b] School of Materials Science and Engineering, Georgia Institute of Technology, Atlanta, Georgia, 30332, United States

Novel branched azobenzene-modified POSS nanostructures that are able to form uniform, ultrathin films, and undergo light induced *trans-cis* isomerization have been prepared.